The Korean Journal of Ceramics, **6**[1] 64-67 (2000)

Ferroelectric Properties and Comparison between PZT/IrO_2 and PZT/Ir

Min-Seok Jeon, Hee-Soo Lee*, Il-Doo Kim and Duck-Kyun Choi**

Department of Inorganic Materials Engineering, Hanyang University, Seoul 133-791, Korea
**Material Analysis Team, Korea Testing Laboratory, Division of KITECH, Seoul 152-053, Korea*
***Department of Materials Science and Engineering, Korea Advanced Institute of Science and Technology, Taejon 305-701, Korea*
(Received September 23, 1998)

Reactively sputtered $Pb(Zr,Ti)O_3$ (PZT) films on IrO_2 and Ir were evaluated with particular consideration on interface properties. The IrO_2 and Ir were previously annealed at 650°C in O_2 or N_2 atmosphere, respectively. There was no appreciable roughening in the interface of the PZT/IrO_2 respective to that of the PZT/Ir; the rms roughness of IrO_2 and Ir was about 3 nm and 10 nm, respectively. The ferroelectric properties of the PZT/IrO_2 were found to be better than that of the PZT/Ir; however, the leakage current of the PZT/IrO_2 was slightly larger than that of the PZT/Ir. The PZT/IrO_2 thin films did not exhibit any fatigue up to 10^{11} cycles; the P^*r - $P^{\wedge}r$ value decreased only from 16.6 to 14 μC/cm^2 until 10^{12} polarization reversals. On the other hand, although thin IrO_2 layer was formed between PZT and Ir, the PZT/Ir thin films began to undergo fatigue after 10^9 polarization reversals.

Key words: $Pb(Zr,Ti)O_3$, IrO_2, Ir, Diffusion barrier, Pb diffusion, Interface, Fatigue, Leakage current

I. Introduction

Ferroelectric lead zirconate titanate ($Pb(Zr,Ti)O_3$, PZT) has been actively researched for ferroelectric random access memory (FRAM) in conjunction with the progress of device technology.[1,2] As these devices undergo a large number of read/write cycles when they are used in a destructive readout mode, they are required to have a long term reliability under various operating conditions. Considering high switching endurance, fatigue must be minimized to realize the integration of high density FRAM with CMOS underlayer. To improve this property, many studies have been carried out in terms of crystalline quality, microstructure or electrode materials.[3,4] There are several factors pinning domain walls: electronic charge trapping, oxygen vacancies or other defects. However, it is nearly impossible to discriminate between these mechanisms and there is not yet an independent mechanism. There are two present trends to improve the reliability of ferroelectric PZT thin films, which are intended for bulk (Bi-based layered perovskite, $SrBi_2Ta_2O_9$) and interface aspects. For the latter, the electrode materials have a crucial influence on the electrical properties such as polarization versus coercive field (P-E) hysteresis, polarization fatigue and leakage characteristics. A noble metal alike Pt, conducting oxide electrodes such as RuO_2[5,6], LSCO[7] or $SrRuO_3$[8,9] and hybrid electrodes [10,11] have been studied. Recently, IrO_2 has been researched for application to the capacitor storage node along with Ir[12,13] and, however, there is not sufficient data of PZT on these two electrodes to date.

In this study, the electrical properties between PZT and Ir-based electrode (IrO_2 and Ir) were investigated. The bottom electrodes were thermally treated at 650°C by rapid thermal annealing (RTA). The fatigue and leakage properties were characterized and compared between PZT/IrO_2 and PZT/Ir by considering particularly the interface properties.

II. Experimental Procedure

200 nm PZT thin films were deposited at 550°C by dc reactive sputtering using multiple 3-inch metal targets. The working pressure was 10 mTorr and the Ar/O_2 ratio was 95/5. IrO_2 (100 nm) and Ir (110 nm) electrodes were deposited by sputtering method on p-type Si wafer with a SiO_2 layer (100 nm) at room temperature. These two electrodes were annealed at 650°C by rapid thermal annealing (RTA). Top Pt electrodes were deposited by dc sputtering at room temperature and patterned with a metal shadow mask (200 mm in diameter). The crystallinity of the films was examined using an X-ray diffractometer (MAC Science). The surface roughness of the bottom electrodes and the PZT films were obtained from atomic force microscopy (AFM). The depth profiles of each elements and the interface were analyzed by auger electron spectroscopy (AES) and transmission electron microscopy (TEM), respectively. The

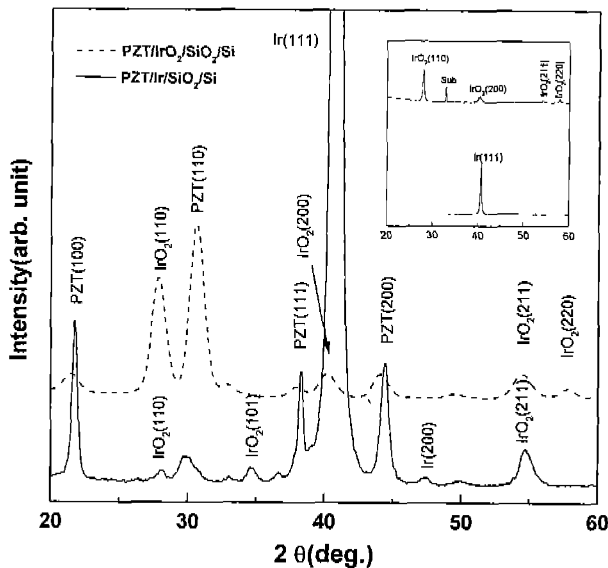

Fig. 1. X-ray diffraction patterns of PZT thin films deposited on IrO_2 and Ir bottom electrodes. The Ir and IrO_2 were annealed at 650°C by rapid thermal annealing (RTA). XRD results of the electrodes are also shown in the box.

fatigue and leakage characteristics of the PZT thin films were investigated using a RT66A standard ferroelectric tester (Radiant Technologies) and HP41-45B semiconductor parameter analyzer, respectively. All the measurements were carried out at room temperature.

III. Results and Discussion

Fig. 1 shows the XRD patterns of the PZT (Zr/Ti=52/48) films and the bottom electrodes. As-deposited IrO_2 and Ir bottom electrodes were annealed at O_2 and N_2 atmosphere, respectively. The substrates were maintained at 650°C in a RTA system. There was not any reduction on IrO_2 surface from no indication of Ir peaks. In addition, when the Ir electrodes were annealed in N_2 atmosphere, they did not oxidize and had well oriented (111) direction. When the PZT films were deposited on IrO_2, they had a dominant (110) orientation. (100) and (111) oriented PZT thin films were obtained on the Ir electrodes. There were additional IrO_2 peaks in the XRD patterns of the PZT/Ir, which tells that IrO_2 layer was formed at the PZT/Ir interface during the PZT deposition. The peak shape of the PZT/Ir was sharp relative to the PZT/IrO_2, which is probably due to the fine grain of the PZT films on IrO_2.

The surface topology of the annealed electrodes and the PZT films is illustrated in Fig. 2. The rms roughness of IrO_2 and Ir was about 3 nm and 10 nm, respectively; as-deposited IrO_2 and Ir had almost similar surface roughness of 1 nm. This surface roughening is ascribed to the grain growth of the crystallites through the annealing. In this study, Ir had very larger surface roughness than IrO_2 at the same annealing temperature. This significant change in the surface morphology of Ir after annealing can deteriorate the

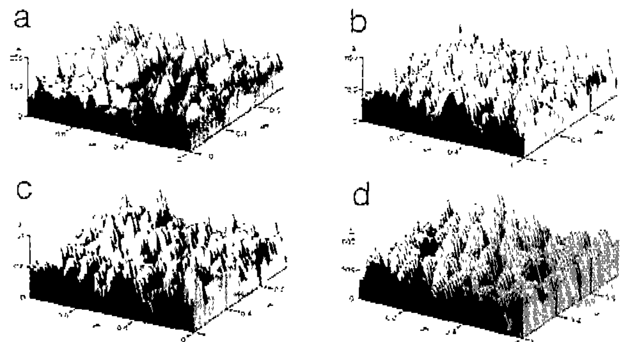

Fig. 2. Atomic force microscopy (AFM) images of (a) IrO_2, (b) Ir, (c) PZT/IrO_2 and (d) PZT/Ir.

electrical properties of PZT films. On the whole, the surface morphology of the PZT films was similar regardless of the bottom electrodes and the rms roughness was about 10 nm and 10.6 nm for PZT/IrO_2 and PZT/Ir, respectively. This similar surface roughness indicated that the surface morphology of the PZT thin films were controlled by the deposition itself more than the bottom electrode in this study

The fatigue characteristics of the PZT thin films deposited at identical conditions on IrO_2 and Ir is illustrated in Fig. 3. The alternating square pulse with a voltage of 5 V high and a frequency of 10 MHz was applied to both PZT thin film capacitors at room temperature. Considering their reasonable value in the difference between switched and non-switched polarization (P^*r-$P^\wedge r$), it is judged that both PZT thin film capacitors may be applied for the capacitor cell of FRAM. The PZT/Ir film began to exhibit some fatigue after 10^9 cycling, while the PZT/IrO_2 film did not show nearly any fatigue until 10^{11} cycling. The polarization versus coercive field plot (P-E hysteresis) before and after the fatigue test is also illustrated in the boxes of Fig. 3. There was no significant change in the P-E hysteresis of the PZT/IrO_2 and the

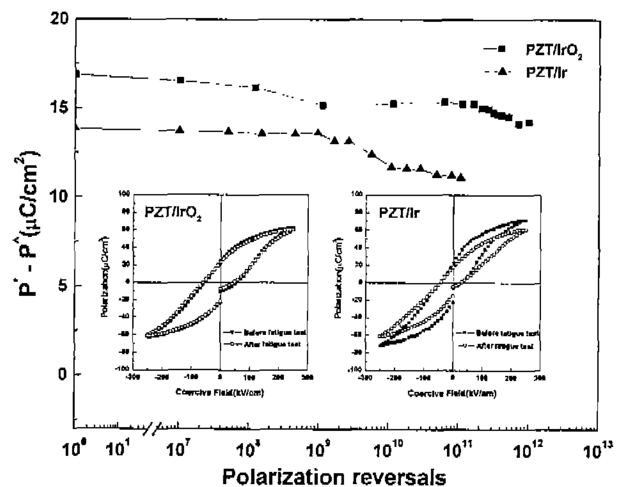

Fig. 3. Fatigue characteristics of PZT films with bottom electrodes. Polarization-coercive field (P-E) hysteresis loops of the PZT films on IrO_2 and Ir were obtained before and after the fatigue test.

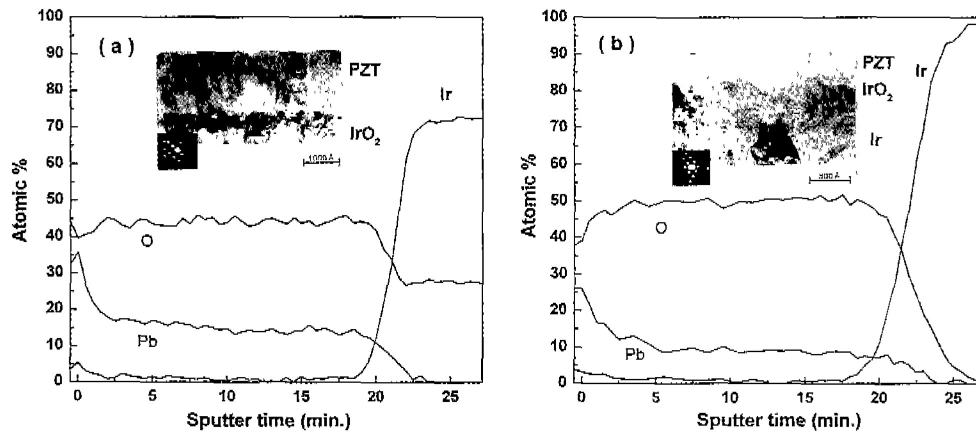

Fig. 4. Auger electron spectroscopy (AES) depth profiles of (a) PZT/IrO_2 and (b) PZT/Ir and cross-sectional transmission electron microscopy (TEM) images. Selected area diffraction (SAD) patterns was from the IrO_2 and Ir region. It is shown that there is IrO_2 layer between PZT and Ir and this layer is formed during the PZT deposition.

remanent polarization before the test was 25 μC/cm.^{2} On the other hand, the polarization of the PZT/Ir slightly decreased after the fatigue test. The coercive field of the PZT/IrO_2 is somewhat larger than that of the PZT/Ir. This is ascribed to the small difference in the grain size and the XRD patterns; (111) oriented PZT usually shows more slim P-E hysteresis loop than (110) oriented one. The difference in the fatigue endurance of the two capacitors was discussed mainly by considering interfacial properties; in addition, there are minor effects alike the difference in crystalline orientation and grain size. From the XRD patterns (Fig. 1), there were IrO_2 peaks in the PZT/Ir films. It is suggested that the IrO_2 is spread along the PZT/Ir interface since it is formed during the PZT deposition. This IrO_2 interlayer was confirmed by a TEM photograph (Fig. 4). The Pb diffusion can be compared between PZT/IrO_2 and PZT/IrO_2/Ir from the AES depth profiles as shown in Fig. 4. There is also probable diffusion of other elements. Pb elements probably diffused into the bottom electrode in spite of the formation of IrO_2 phase between PZT and Ir, while PZT/IrO_2 did not showed such Pb diffusion. The Pb profile in the PZT/IrO_2/Ir was broader than that of PZT/IrO_2, which illustrates the possibility of the Pb diffusion. Considering this result, the IrO_2 interfacial layer is too thin to block the Pb diffusion.[13] Pb diffusion unfortunately forms Pb-deficient layer at the interface and this layer resulted in the decrease of P^*r - $P^{\wedge}r$ in PZT/Ir. In addition, the thin IrO_2 layer may be not adequate for a sink for oxygen vacancies in PZT films and the high surface roughness of Ir electrode may also deteriorate the fatigue characteristics. On the other hand, the PZT/IrO_2 had more flat interface than the PZT/Ir, which was coincident with AFM result. The PZT films had a well-grown columnar structure and there was not any interfacial layer between PZT and IrO_2.

Fig. 5 shows the leakage current versus applied voltage curves of the PZT film on IrO_2 and Ir. The leakage current in the PZT/IrO_2 and PZT/Ir thin film capacitors was 1.2×10^{-6} A/cm^2 and 4×10^{-7} A/cm^2 at 1.5 V, respectively; the thickness of the PZT films was 200 nm. The PZT/Ir thin films did not show a significant variation between 0 and 5 V. The usual PZT/Pt thin films have a flat region of I-V curve at low electric field and show a considerable leakage current with voltage at high field region. With difference from this, the small increase in the leakage current of the PZT/Ir is attributed to the change of the interface properties resulting from the formation of thin IrO_2 layer; that is, the thin IrO_2 interlayer may make a relaxing effect on the leakage current. On the other hand, the leakage current in the PZT/IrO_2 gradually increased up to an applied voltage of 3.5 V and then it abruptly increased. It is speculated that somewhat large current of the PZT/IrO_2 is related to both grain boundary and low interfacial potential. The leakage current increases with the decrease of grain size. Although there is an IrO_2

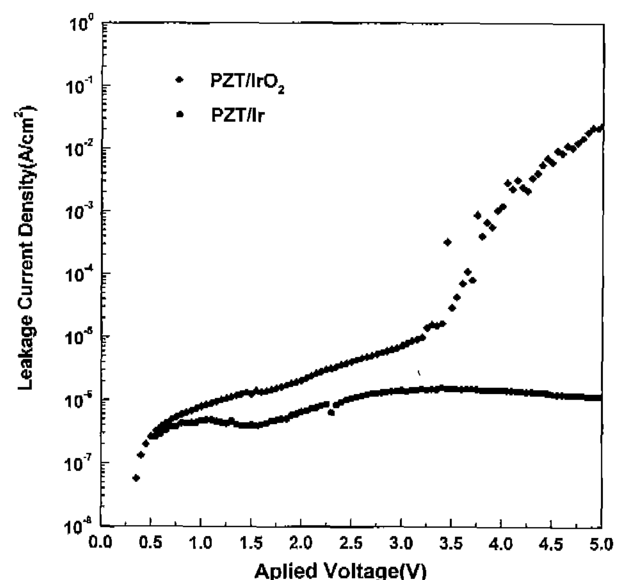

Fig. 5. Leakage current vs. applied voltage curves of the PZT thin films deposited on thermally treated IrO_2 and Ir electrodes.

layer at the PZT/Ir interface, it is suggested that this interface (PZT/IrO_2) formed during the PZT deposition is different from the PZT/IrO_2/SiO_2/Si.

IV. Conclusions

The effectiveness of IrO_2 and Ir as the electrode for PZT was evaluated. IrO_2 and Ir were annealed at 650°C by RTA. The PZT films were reactively sputtered at 550°C. AFM and TEM analysis showed that there was no appreciable roughening in the PZT/IrO_2 interface respective to the PZT/Ir interface. In case of the PZT/Ir thin films, IrO_2 layer was formed by the oxidation of Ir electrode during PZT deposition process. The PZT/IrO_2 films exhibited nearly no fatigue up to 10^{11} polarization reversals. From the depth profiles of the PZT/IrO_2 and PZT/Ir, Pb diffusion was observed through the PZT/Ir interface despite the thin IrO_2 layer formation. Opposite to the PZT/IrO_2, the fatigue in the PZT/Ir began just after 10^9 polarization reversals. This is attributed to the probable formation of Pb-deficient layer between PZT and Ir along with the rough interface between them. The PZT/Ir had slightly smaller leakage current than the PZT/IrO_2.

References

1. S. S. Dana, K. F. Etzold and J. Clabes, "Crystrallization of Sol-Gel Derived Lead Zirconate Titanate Thin Films," *J. Appl. Phys.*, **69**(8), 4398-4403 (1991).
2. S. Sinharoy, H. Buhay, D. R. Lampe and M. H. Rrancombe, "Integration of Ferroelectric Thin Films into Nonvolatile Memories," *J. Vac. Sci. Technol.*, **10**(4),1554-1561 (1992).
3. H. N. Al-Shareef, A. I. Kingon, X. Chen, K. R. Bellur and O. Auciello, "Contribution of Electrodes and Microstructures to the Electrical Properties of Pb(Zr,Ti)O_3 Thin Film Capacitors," *J. Mater. Res.*, **9**(11), 2968-2975 (1994).
4. D. J. Taylor, J. Geerse and P. K. Larsen, "Fatigue of Organometallic Chemical Vapor Deposited Pb(Zr,Ti)O_3 thin films with Ru/RuO_2 and Pt/Pt Electrodes," Thin Solid Films, **263**, 221-230 (1995).
5. H. Maiwa, N. Ichinose and K. Okazaki, "Preparation and Properties of Ru and RuO_2 Thin Film Electrodes for Ferroelectric Thin Films," *Jpn. J. Appl. Phys.*, **33**(9B), 5223-5226 (1994).
6. D. P. Vijay and S. B. Desu, "Electrodes for Pb(Zr,Ti)O_3 Ferroelectric Thin Films," *J. Electrochem. Soc.*, **140**(9), 2640-2645 (1993).
7. R. Dat, D. J. Lichtenwalner, O. Auciello and A. I. Kingon, "Polycrystalline $LaSrCoO_3$/Pb(Zr,Ti)O_3/$LaSrCoO_3$ Ferroelectric Capacitors on Platinazed Silicon with no Polarization Fatigue," *Appl. Phys. Lett.*, **64**(20), 2673-2675 (1994).
8. C. B. Eom, R. B. Van Dover, J. M. Philips, D. J. Werder, J. H. Marshall, C. H. Chen, R. J. Cava and R. M. Fleming, "Fabrication and Properties of Epitaxial Ferroelectric Heterostructures with ($SrRuO_3$) Isotropic Metallic Oxide Electrode," *Appl. Phys. Lett.*, **63**(18), 2570-2572 (1993).
9. M. Hiratani, C. Okazaki, K. Imagawa and K. Takagi, "$SrRuO_3$ Thin Films Grown under Reduced Oxygen Pressure," *Jpn. J. Appl. Phys.*, **35**(12A), 6212-62126 (1996).
10. H. N. Al-Shareef, K. R. Bellur, A. I. Kingon and O. Auciello, "Influence of Platinum Interlayers on the Electrical Properties of RuO_2/Pb(Zr,Ti)O_3/RuO_2 Capacitor Heterostructures," *Appl. Phys. Lett.*, **66**(2), 239-241 (1995).
11. M. S. Jeon, J. B. Lee and D. K. Choi, "Electrical Characterization of Ferroelectric Pb(Zr,Ti)O_3 Thin Films Deposited on Pt-Coated RuO_2 Electrodes," *Jpn. J. Appl. Phys.*, **37**(6A), 3391-3395 (1998).
12. T. Nakamura, Y. Nakao, A. Kamisawa and H. Takasu, "Preparation of Pb(Zr,Ti)O_3 Thin Films on Ir and IrO_2 Electrodes," *Jpn. J. Appl. Phys.*, **33**(9B), 5207-5210 (1994).
13. M. Shimizu, H. Fujisawa, S. Hyodo, S. Nakashima, H. Niu, H. Okino and T. Shiosaki, "Pb(Zr,Ti)O_3 Thin Film Deposition on Ir and IrO_2 Electrodes by MOCVD," *J. Kor. Phys. Soc.*, **32**, S1349-1352 (1998).